

DOI: 10.5586/asbp.3486

**Publication history**

Received: 2015-08-07

Accepted: 2016-01-25

Published: 2016-03-18

**Handling editor**

Elżbieta Bednarska-Kozakiewicz,  
Faculty of Biology and  
Environmental Protection,  
Nicolaus Copernicus University  
in Toruń, Poland

**Authors' contributions**

EWC: research designing; EWC,  
MC: microscopic analysis,  
writing the manuscript,  
observation of flowering,  
collection and analysis of nectar;  
photographs: MC

**Funding**

This research was supported by  
the Polish Ministry of Science  
and Higher Education as part of  
the activities of the University of  
Life Sciences in Lublin.

**Competing interests**

No competing interests have  
been declared.

**Copyright notice**

© The Author(s) 2016. This is an  
Open Access article distributed  
under the terms of the [Creative  
Commons Attribution License](#),  
which permits redistribution,  
commercial and non-  
commercial, provided that the  
article is properly cited.

**Citation**

Weryszko-Chmielewska E,  
Chwil M. Flowering biology and  
structure of floral nectaries in  
*Galanthus nivalis* L. Acta Soc  
Bot Pol. 2016;85(1):3486. [http://  
dx.doi.org/10.5586/asbp.3486](http://dx.doi.org/10.5586/asbp.3486)

**Digital signature**

This PDF has been certified using digital  
signature with a trusted timestamp to  
assure its origin and integrity. A verification  
trust dialog appears on the PDF document  
when it is opened in a compatible PDF  
reader. Certificate properties provide  
further details such as certification time  
and a signing reason in case any alterations  
made to the final content. If the certificate  
is missing or invalid it is recommended to  
verify the article on the journal website.

## ORIGINAL RESEARCH PAPER

# Flowering biology and structure of floral nectaries in *Galanthus nivalis* L.

Elżbieta Weryszko-Chmielewska\*, Mirosława Chwil

Department of Botany, University of Life Sciences in Lublin, Akademicka 15, 20-950 Lublin,  
Poland

\* Corresponding author. Email: [elzbieta.weryszko@up.lublin.pl](mailto:elzbieta.weryszko@up.lublin.pl)

**Abstract**

In Poland *Galanthus nivalis* L. is partially protected. The flowers of this species are one of the first sources of nectar and pollen for insects from February to April. The aim of this study was to present the flowering biology as well as the topography, anatomical, and ultrastructural features of the floral nectary. The flower lifespan, the breeding system, and the mass of pollen and nectar produced by the flowers were determined. Examination of the nectary structure was performed using light, fluorescence, scanning and transmission electron microscopy. The flower of *G. nivalis* lives for about 30 days. The stamens and pistils mature simultaneously and during this time nectar is secreted. The anthers of one flower produced the large amount of pollen (4 mg). The breeding system of *G. nivalis* was found to be characterized by partial self-compatibility, outcrossing, and xenogamy. The nectary is located at the top of the inferior ovary. The nectary epidermal cells are characterized by striated cuticular ornamentation. Initially, the secreted nectar formed vesicle-like protuberances under the cuticle. The epidermal and parenchymal cells contain numerous plastids, mitochondria, dictyosomes, ER cisterns, and vesicles fused with the plasmalemma, which indicates granulocrine nectar secretion.

**Keywords**

*Galanthus nivalis*; flower; breeding system; pollen mass; nectar production; structure of nectary

**Introduction**

The area of occurrence of *Galanthus nivalis* L. includes Western, Central, and Eastern Europe, the mountains of the Crimea and the Caucasus as well as Minor Asia. *G. nivalis* is a species characteristic of Southern European mixed deciduous forests, particularly dry-ground forests of the association *Carpinion betuli illyricum* found in the Balkan Peninsula [1]. This species is considered to be an indicator plant in phenological studies in many European countries: Austria, Bosnia and Herzegovina, Croatia, the Czech Republic, Germany, Lithuania, the Netherlands, Slovakia, and the UK, in which the “first flowers open” stage is taken into consideration [2].

In Poland *G. nivalis* is found in the south, in lower mountainous locations, in the central part of the country as well as in the Lublin region (Lubelszczyzna) and in the Wielkopolska region. It is worth stressing that the northern limit of the range of *G. nivalis* runs through Poland where it is a species characteristic of mesophilic deciduous forests of the order *Fragetalia sylvaticae* [3]. *Galanthus nivalis* was fully protected in Poland during the period 1946–2014 as a rarely encountered species. Since 2014 it has been partially protected [4].

In Poland the flowering period of *G. nivalis* lasts from February to April [3]. After winter, the flowers of *G. nivalis* are one of the first sources of nectar and pollen for insects. The bell-shaped flowers of this species exhibit structural adaptations to the thermal conditions prevailing in early spring [5,6]. The colored markings in the form of green spots and stripes on the tepals as well as the scent and nectar produced by the flowers are adaptations to entomogamy [6,7].

The flowers of monocot species are highly diverse in terms of the location and structure of nectaries [8–10]. Some representatives of the Amaryllidaceae family, e.g., *Narcissus* [11], have septal nectaries, while in others the nectaries are located on the tepals [10,12]. In the literature, no detailed data can be found about the structure of the *G. nivalis* nectary. Szafer and Wojtusiakowa [13] reported that in this species nectar is secreted via a nectary disk located on the surface of the inferior ovary. Daumann [8] found two types of nectaries in this flower: one on the tepals and the other one, which is disk-shaped, at the base of the flower. Kugler [7] noticed that the thin-walled tissues of the nectary of *G. nivalis* were often chewed by insects visiting its flowers. In our previous study, we found that the floral nectary in *G. nivalis* was located at the top of the inferior ovary between the base of the tepals and the style and formed a bright layer contrasting with the green receptacle fused with the ovary. This work is a continuation of our earlier study on the micromorphology and anatomy of some floral structures of this species [6].

Since *G. nivalis* is a species that attracts interest from the point of view of phenology, whose flowering is studied in the aspect of its response to climate warming [14,15], we undertook a study on the ecology of flowering of this species in the conditions of central-eastern Poland. The aim of the research presented in this paper was to determine the lifespan of the *G. nivalis* flower, stigma receptivity, the period of pollen and nectar presentation as well as the mass of pollen and nectar, and also to evaluate the breeding system of this species. A large part of this paper is devoted to the results of the investigations of the topography, micromorphology, and the anatomical and ultrastructural features of the nectary. This study was undertaken to explain the divergent data found in the literature as regards the location of the nectary in the *G. nivalis* flower and to fill the gap in the information concerning the structure of the nectary gland in this species.

## Material and methods

### The flower stages in the study

*Galanthus nivalis* L. plants were supplied by the Botanical Garden of the Maria Curie-Skłodowska University in Lublin. We selected 10 buds on each of the experimental plants planted in three districts of the city in order to investigate the flower lifespan and stigma receptivity. The bud swell stage was considered to be the beginning of flowering. We conducted a morphometric analysis of the individual parts of the flower. We determined the nectary size and stigma receptivity at different flower development stages: closed bud (I), bud swell (II), bud burst (III), partially open flower (IV), and fully open flower (V; Fig. 1d–h). At the individual stages, we measured the perianth length as well as the nectary diameter and height ( $N = 16$ ).

### Stigma receptivity and breeding system

We examined stigma receptivity using the Peroxtesmo Ko test which causes blue or bluish green coloration within two minutes after a reaction with peroxidase present in the tissues of a receptive stigma [16]. The characteristics of the breeding systems and the outcrossing level of *G. nivalis* were determined using the method recommended by Cruden, as described by Dafni [16], after the determination of the number of pollen grains (P;  $N = 6$ ) and ovules (O) produced by the flower ( $N = 20$ ).

### Study of nectar and pollen grains

The mass of nectar was determined at bud burst (III) and fully open flower (V) stages using the method by Jabłoński [17]. For the analysis, we collected 6 nectar samples from 8–16 flowers at either stage. The nectar sugar content was measured using a refractometer.

The mass of pollen produced by a stamen was measured using the method by Warakomska [18]. Samples ( $N = 10$ ) included 50 mature stamens collected at bud swell stage (II) before the onset of pollen shed.

### Nectary structure

To examine the nectary structure, flowers were collected at the stages II and V. To perform preliminary analysis by light microscopy, hand-made longitudinal sections of fragments of the ovary with a nectary were prepared and stained with Lugol's solution and Sudan III in order to detect starch and lipids [19].

### Permanent microscope slides

Nectaries sampled from fresh flowers were fixed in 4% glutaraldehyde at a temperature of 21°C for 6 hours and in 0.1 M phosphate buffer, pH 7.0, at 4°C for 24 hours. The samples were washed with phosphate buffer and treated with 1% OsO<sub>4</sub> at 0°C for 2 hours. Nectary fragments were stained with a 0.5% water solution of uranyl acetate. Next, the plant material was dehydrated in ethanol, embedded in Spurr Low Viscosity resin, and polymerized at 60°C.

### Light microscopy (LM)

For observation of the nectary cells, semi-thin longitudinal 0.8–1- $\mu$ m thick sections were stained with toluidine blue (0.25%) [19] and periodic acid-Schiff's reagent (PAS) staining was also performed [20]. The slides prepared in this way were analyzed under a Nikon Eclipse 400 light microscope.

### Fluorescence microscopy (FM)

After addition of fluorochrome (a 0.01% solution of auramine O) [21], hand-made sections from fresh nectary fragments and semi-thin sections from the fixed material were embedded in a 50% glycerol solution. The observations were carried out under a NIKON Eclipse 90i fluorescence microscope equipped with a fluorescein isothiocyanate – FITC filter (excitation light 465–495 nm), a DAPI filter (365–461 nm), and a barrier filter (wavelength 515–555 nm).

### Transmission electron microscopy (TEM)

Ultrathin 70-nm thick sections were cut with a Reichert Ultracut S microtome. They were stained with an 8% uranyl acetate solution in 0.5% acetic acid for 40 minutes; the sections were washed twice with distilled water (10 minutes) and contrasted with the Reynolds reagent (15 minutes) [22]. The slides were dried after rinsing with water. The nectary cell ultrastructure in the pre-secretory phase and at full nectar secretion was observed under a FEI Tecnai G2 Spirit transmission electron microscope.

## Scanning electron microscopy (SEM)

After dehydration in increasing concentrations of acetone, i.e., 15, 30, 50, 70, 90, and 99.5% (anhydrous acetone was used twice) for 15 minutes in each concentration, the fixed plant samples were critical-point dried in liquid CO<sub>2</sub> in an Emitech K850 dryer and sputter-coated with gold using an EMITECH K550X sputter coater. The analysis of the surface of the nectary epidermis was performed under a Tescan Vega II LMU scanning electron microscope.

## Results

### Flowering period

In 2015 the flowering of *G. nivalis* lasted from 18 February to 23 March. Observations carried out simultaneously in three parts of the city produced similar results. The average flower lifespan was 31 days (Fig. 2). On the first day of flowering, when swollen buds were observed (Fig. 1e), the mean daily temperature was  $-0.8^{\circ}\text{C}$ . The beginning of senescence of the inner tepals, which took place at a temperature of  $+5.3^{\circ}\text{C}$ , was considered to be the end of flowering. During the time of flowering, the temperature increased to  $+8.5^{\circ}\text{C}$  and on most days it remained in the range of  $4\text{--}7^{\circ}\text{C}$  (Fig. 2).

We found stigmatic receptivity, using the Proxtesmo Ko test (Fig. 1j,k), already at the closed bud stage (Fig. 1d,e) and it continued until the time of senescence of the outer tepals (25 days). Over the same time, we observed anther dehiscence and the presentation of pollen; we also found scent emission by the tepals (sensory method) and nectar secretion (Fig. 2). Senescence of the outer tepals occurred 5 days earlier than in the case of the inner tepals, and the scent emitted by the inner tepals was clearly detectable even when the outer tepals had already lost their attractive appearance. Senescence of the tepals began on 15 March and in some flowers the whole perianth with the stamens fell off already after 8 days, while in some other ones it remained desiccated for 27 days (until 10 April). During this period, the temperature maintained at about  $13^{\circ}\text{C}$  for several days and different sized fruit primordia formed from the ovary of the pistil.

### Floral morphology and pollen production

The bell-shaped flowers of *G. nivalis* were composed of 3 white boat-shaped outer tepals with a length of about 20 millimeters and three inner tepals about 10 mm long (Tab. 1). The inner tepals were marked with V-shaped green marks on the abaxial surface and green stripes on the adaxial surface. On cloudy weather the tepals most frequently remained folded, whereas on sunny days we could observe substantial opening of the perianth, in particular the outer tepals (Fig. 1a–c). The androecium consisted of six stamens with an average length of 7 mm, arranged in two whorls. The large anthers accounted for 80% of the stamen length (Tab. 1). The pistil had an inferior ovary with an average height of 4.34 mm and a style that reached a length of 8 mm and protruded above the anthers (Fig. 1i). The distance between the stigma and the apical part of the anthers was 1.5–2 mm. We found different numbers of ovules (33–49) in the ovaries.

The mass of pollen per stamen was 0.66 mg, while the average mass of pollen produced by one flower was 4 mg (Tab. 1). We determined the average number of pollen grains produced per stamen, which was 62 850. At an air temperature of  $7\text{--}8^{\circ}\text{C}$ , we observed bees collecting nectar and pollen from the *G. nivalis* flowers (Fig. 1c). Pollen loads formed from the pollen of this species were orange.



**Fig. 1** Flowers and fragments of the floral parts of *Galanthus nivalis* (i–k LM; m FM; l, n, o SEM). a–c Campanulate flowers with visible green marks on the tepals. d–h Different flower development stages: closed bud (stage I; d); bud swell (stage II; e); bud burst (stage III; f); beginning of flowering (stage IV; g); flower open (stage V; h). i Flower at bud swell after cutting tepals (stage II); the nectary is visible on the surface of the inferior ovary located between the base of the stamens and the base of the pistil's style (arrow). j Pistil's style; visible a receptive stigma after using Peroxtesmo Ko test (two arrows) and pollen grains (arrowheads) on the style surface (stage II). k Papillae on the stigma (asterisks); Peroxtesmo Ko test. l Papillae on the abaxial surface of the epidermis of the inner tepals; visible longitudinal cuticular striae; SEM. m Cross sectional view of the inner tepal. n Characteristic ribs and numerous stomata (double-headed arrow) in the adaxial epidermis of the inner tepals. o Stoma and cuticular ornamentation consisting of twisted striae on the surface of other epidermal cells (inner tepals).

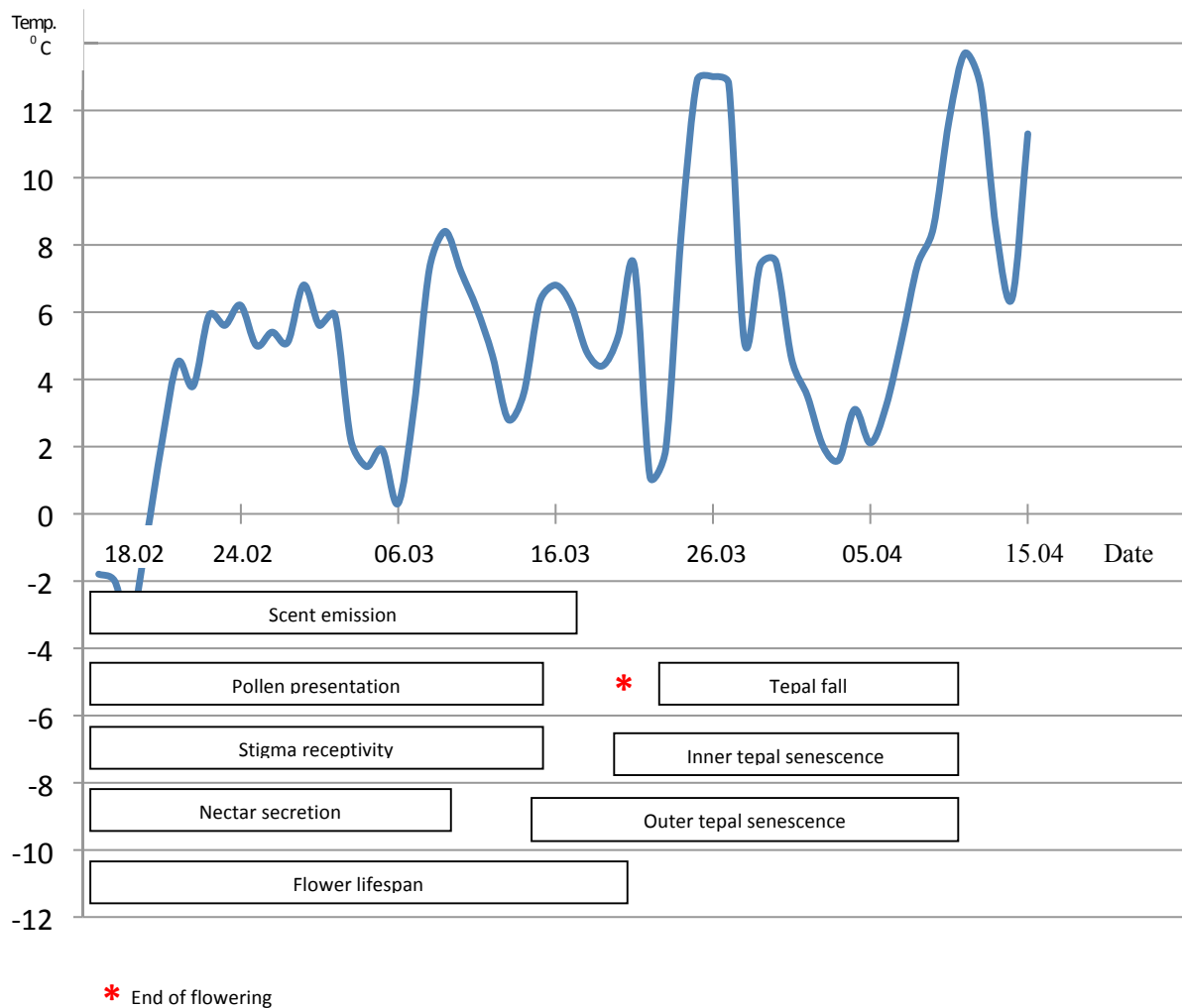


Fig. 2 Different stages of anthesis (31 days) of *Galanthus nivalis* flowers.

Tab. 1 Morphological characters of *Galanthus nivalis* flowers and pollen weight per flower.

Investigated character		Min.–max.	Mean	SD
Outer tepal length	mm	17.0–24.0	20.91	2.07
Inner tepal length		8.5–12.0	10.34	1.77
Anther length		4.0–6.5	5.53	0.62
Stamen length		6.0–7.5	6.97	0.53
Style length		6.5–9.5	7.98	0.76
Ovary height		3.0–6.0	4.34	0.99
Pollen mass per stamen	mg	0.61–0.73	0.66	0.06
Pollen mass per flower		3.66–4.38	3.96	0.37

**Tab. 2** Bud or outer tepal length and nectary size at different development stages of *Galanthus nivalis* flowers; *N* = 16.

Nectary development stages	Bud / outer tepal length (mm)	Nectary diameter (mm)	Nectary height (µm)
	Mean ±SD		
I	13.1 ±1.8	1.79 ±0.20	390.5 ±4.0
II	16.2 ±1.4	1.86 ±0.31	438.3 ±59.5
III	16.9 ±0.9	1.92 ±0.20	441.0 ±70.6
IV	18.8 ±1.7	1.95 ±0.26	448.4 ±37.4
V	21.8 ±1.8	1.96 ±0.21	484.1 ±71.2

## Nectary size and nectar production

We examined the size of the nectaries at different flower development stages (Fig. 1d–h). We found that at the successive stages (I–V) the nectary size increased with the elongation of the perianth. The perianth length (13.1 mm) at closed bud stage (I) was 60% of the perianth length at stage V (21.8 mm). On the other hand, the nectary diameter at stage I reached as much as 91% of the nectary diameter at fully-open flower stage (1.96 mm). Slightly larger differences in the nectary height were found at different flower opening stages. At stage I, the nectary height was

80% of its height at stage V (484 µm; Tab. 2). The nectar produced in the flower is visible already in a closed bud (stage II) and accumulates in the space between the staminal filaments and the pistil's style, seeping up to the height of the anthers where it comes into contact with their adaxial surface (Fig. 1i). Nectar secretion occurred for about 2/3 of the flowering period (20 days).

We measured the mass of nectar secreted by the flowers bagged to prevent insect visitation at flower development stages III and V. We found much more nectar at stage III (2.66 mg/flower) than at stage V (1.4 mg/flower). At stage III, the nectar was characterized by lower sugar content (16.2%) than at stage V (22.9%), which may be attributable to the gradual loss of water by the nectar with the tepals open. However, due to the larger amount of nectar secreted the mass of sugars offered to insects by the flower at bud burst stage (III) was higher than the mass of sugars in the nectar in open flowers (V; Tab. 3).

## Scent emission

The abaxial (outer) surface of the outer and inner tepals emitting a delicate scent was covered with different sized papillae with characteristic surface striation (Fig. 1l). The adaxial surface of the inner tepals, covered with green striae (Fig. 1b), gave off a much stronger scent. In the cross-sectional view of the inner tepals, ribs were visible on the adaxial surface at the place of occurrence of the green stripes (Fig. 1m). Chloroplasts occurred in the subepidermal layers of parenchyma, while the central part of the tepals, beneath the ribs, was filled with air canals. SEM examination revealed that the epidermal cells covering the adaxial surface were mostly isodiametric and arranged in regular rows. Numerous stomata characterized by a wide opening of the outer cuticular ledges were distributed among them (Fig. 1n,o). The cuticle found on the surface of the epidermal cells formed a characteristic pattern composed of twisted striae (Fig. 1o). The occurrence of numerous stomata is a trait characteristic of tissues emitting a strong odor (osmophores).

**Tab. 3** Nectar production rate in *Galanthus nivalis* flowers.

Flower development stages	Nectar mass mg/flower		Nectar sugar percentage (%)		Nectar sugar mass mg/flower	
	min.–max.	mean ±SD	min.–max.	mean ±SD	min.–max.	mean ±SD
III	1.75–3.67	2.66 ±0.62	15.0–17.5	16.2 ±0.9	0.28–0.59	0.43 ±0.10
V	1.00–2.14	1.40 ±0.32	20.5–28.0	22.9 ±1.8	0.23–0.50	0.32 ±0.08

**Tab. 4** Outcrossing index and breeding system of *Galanthus nivalis*.

Flower characteristics	Results	Values
1. Flower diameter	>6 mm	3
2. Temporal separation of anther dehiscence and stigma receptivity	homogamy	0
3. Spatial positioning of the stigma and anthers	spatially separated	1
<b>OCI (outcrossing index)</b>		<b>4</b>
Breeding system	partially self-compatible, outcrossing, demand for pollinators	

The effects given in the table were calculated according to Dafni [16] tests.

### Breeding system

In the biology of flowering and pollination of plants, functional floral morphology is of great importance, since it allows their sexual systems to be assessed. Tab. 4 presents the characteristics of the flowers of *G. nivalis* that enable the assessment of the breeding system of this species. We calculated the outcrossing index (OCI) based on the flower diameter which was 15–35 mm, depending on perianth opening, and based on the estimation of the temporal and spatial separation of the stigma and anthers. The value of OCI = 4 shows that in *G. nivalis* there is outcrossing and demand for pollinators, but these flowers are partially self-compatible. We also determined the outcrossing level based on the P/O ratio (pollen grains : ovules). The number of pollen grains produced per flower reached 377 100, whereas the average number of ovules per flower was 40. Thus, the P/O ratio is 9427, which indicates xenogamy.

### Nectary micromorphology

The nectary of the *Galanthus nivalis* flowers (Fig. 3a) was located at the top of the inferior ovary between the tepals and the style. The green whitish nectary layer was situated above the green tissues of the ovary (Fig. 3a,b). Nectary tissues formed conical convexities between the filaments and style (Fig. 3e, Fig. 4a) and circular concavities filled with nectar at their bases (Fig. 3a,b).

The outer walls of the nectary epidermal cells viewed in SEM were characterized by striated cuticular ornamentation, which was well visible already in the pre-secretory phase. The undulating, parallel, densely arranged striae in adjacent cells often exhibited varied orientation. They were more loosely arranged at the cell borders (Fig. 4b). In the initial phase of nectar secretion, small vesicle-like convexities appeared among the striae (Fig. 4c). Their number and size increased with the increasing secretory activity of the nectary. The largest vesicles were formed at the borders of adjacent epidermal cells (Fig. 4d,e). The nectar that accumulated under the cuticle led to the formation of convexities and vesicles; the diameter of the latter typically reached 4–15 µm. Locally, the secretion residues formed an irregular layer on the epidermis surface (Fig. 4e). No stomata were observed in the nectary epidermis (Fig. 4a). We also detected nectar secretion within the epidermal cells of the basal part of the filaments, which may imply secretory activity of these floral structures (Fig. 4f).

### Nectary anatomy

Prior to nectar secretion, the nectary epidermis exhibited light green epifluorescence after the treatment with auramine O and the use of the FITC filter (Fig. 3d), or bright blue epifluorescence when the DAPI filter was used (Fig. 3c). As shown by fluorescence microscopy, the layer of the nectary glandular cells was distinguished from the ovary and receptacle tissues by distinct fluorescence (Fig. 3e). The outer walls of the epidermal cells exhibited the presence of a cutinized layer after the application

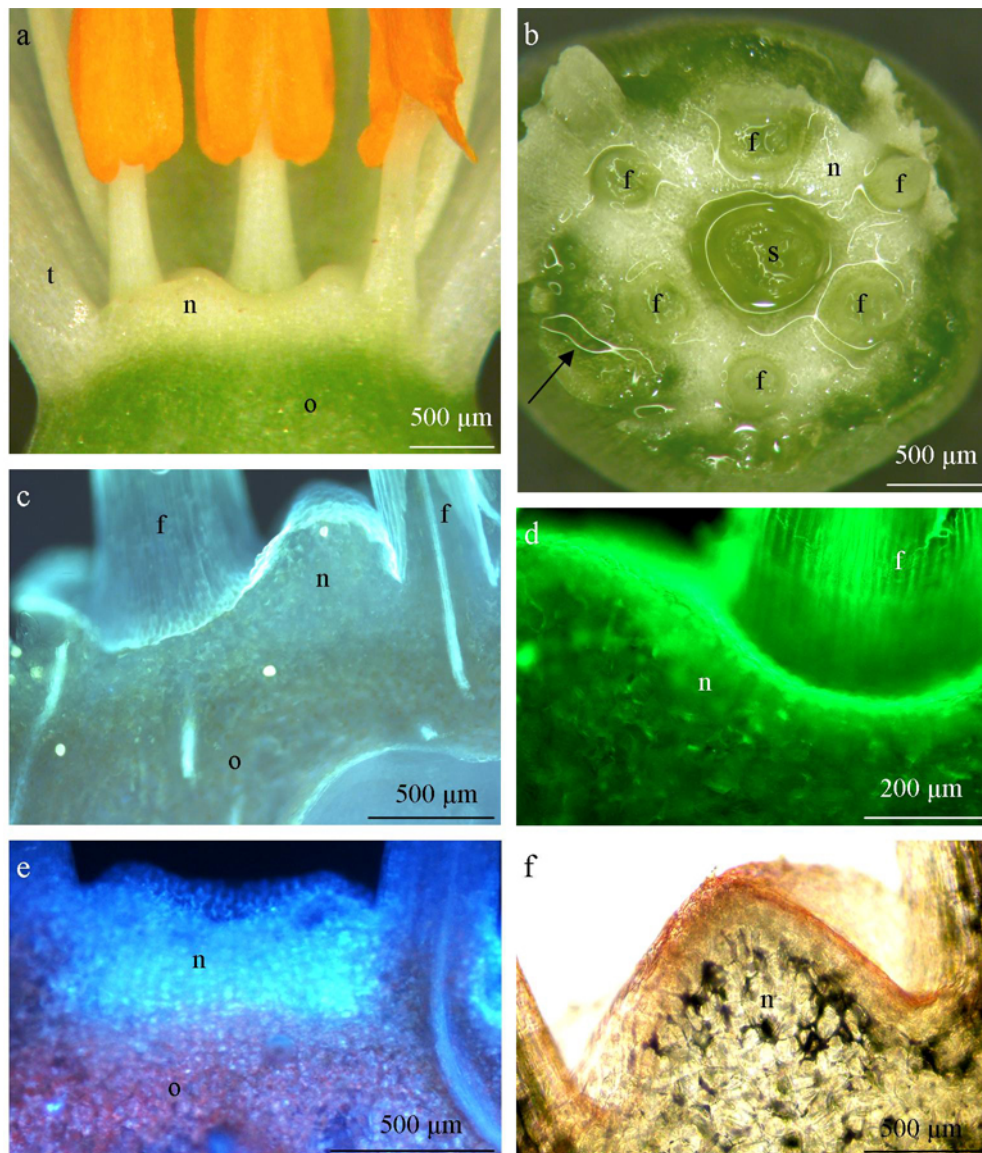


**Fig. 3** Location of the nectary in *G. nivalis* flowers (**a,b,f** LM; **c–e** FM). **a** Nectary located at the apex of the inferior ovary between the bases of the tepals and the style; visible projections of whitish nectariferous tissue between the filaments. **b** Nectary disc with visible shimmering nectar (arrow) accumulated in the concavities surrounding the filaments and the style. **c,d** Longitudinal section of the floral nectary at the initial phase of nectar secretion; visible outer layers of the gland, blue (**c**) and green (**d**) fluorescence of the gland layers (stage II); FM. **e** More intense fluorescence of the nectary layer in an older flower (stage IV); FM. **f** Protrusion of the nectary tissues between the style base and the filament; visible orange-stained cutinized layers. **c–e** After application of the DAPI filter (**c**), after addition of auramine O and using the FITC filter (**d**), autofluorescence (**e**), after treatment with Sudan III (**f**). f – filament; n – nectary; o – ovary; s – style; t – tepal.

of Sudan III (Fig. 3f, Fig. 5c). Nectar drops were visible in the cross sections of fresh nectary tissues (Fig. 5c), which corresponds with our SEM observations. The nectary gland in the flowers of *G. nivalis* is composed of one layer of epidermal cells, 7–10 layers of glandular parenchymal cells, and several layers of sub-nectary parenchyma (Fig. 5a). These layers form a 414–616  $\mu\text{m}$  thick nectary ring (mean 484  $\mu\text{m}$ ).

#### Epidermal cells

The height of the nectary epidermis was 13–21  $\mu\text{m}$ . The outer cell wall was substantially thicker than the anticlinal walls and the periclinal inner wall (Fig. 5a–g, Fig. 6a). The part of the wall in contact with the environment was characterized by intense

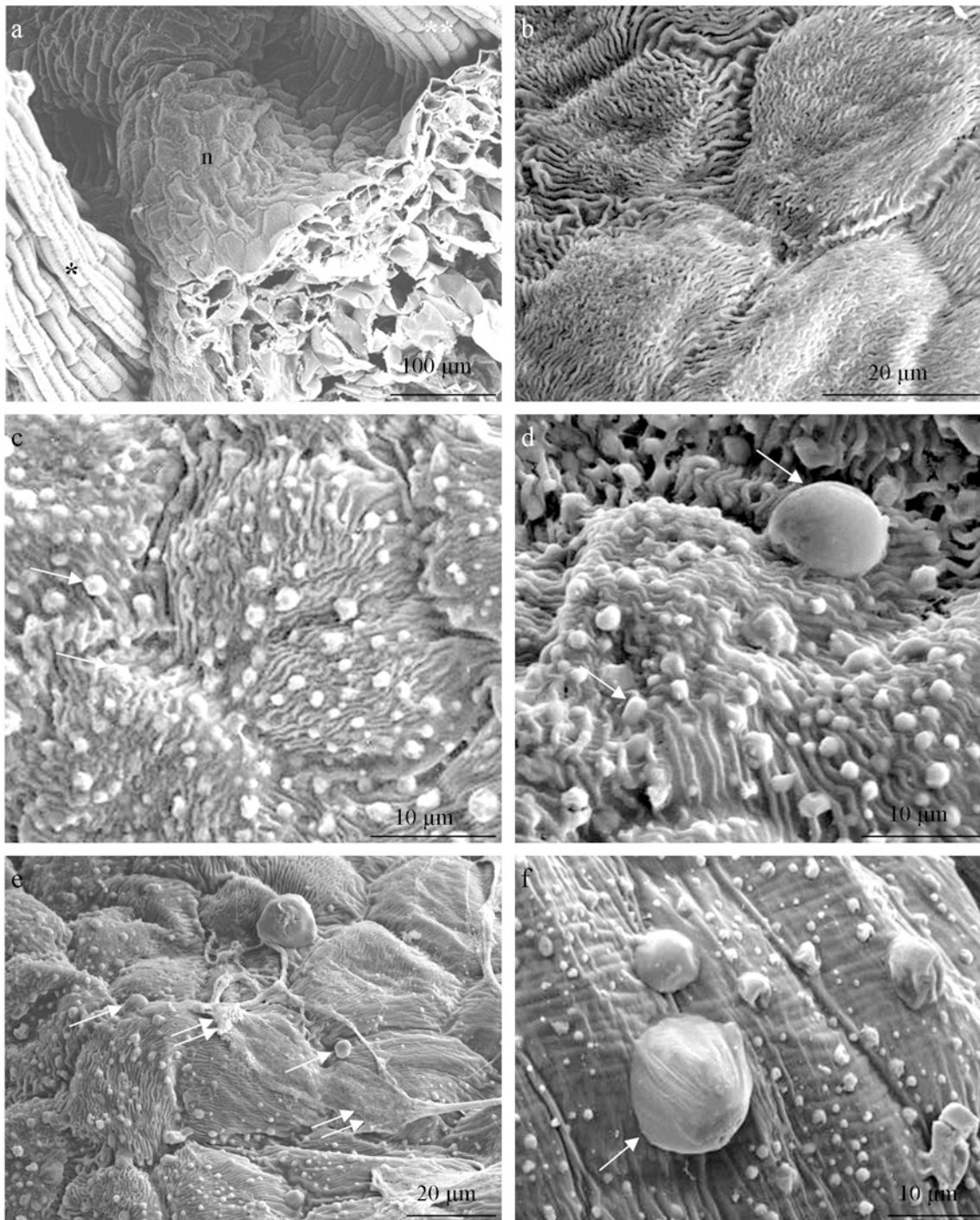


**Fig. 4** Surface of the floral nectary (n) and a filament of *Galanthus nivalis* (SEM). **a** Protrusion of the nectary tissues (n) between the style base (asterisk) and the filament (double asterisk). **b** Surface of nectary epidermal cells with substantially dense cuticular striae (stage I). **c,d** Fragments of the outer walls of nectary epidermal cells with striated cuticular ornamentation and different-sized nectar-containing vesicles (arrows; stage III). **e** Surface of nectary epidermal cells with vesicles (arrows) and secretion residues (double arrow). **f** Surface of filament epidermal cells with nectar-containing vesicles (arrow; stage III).

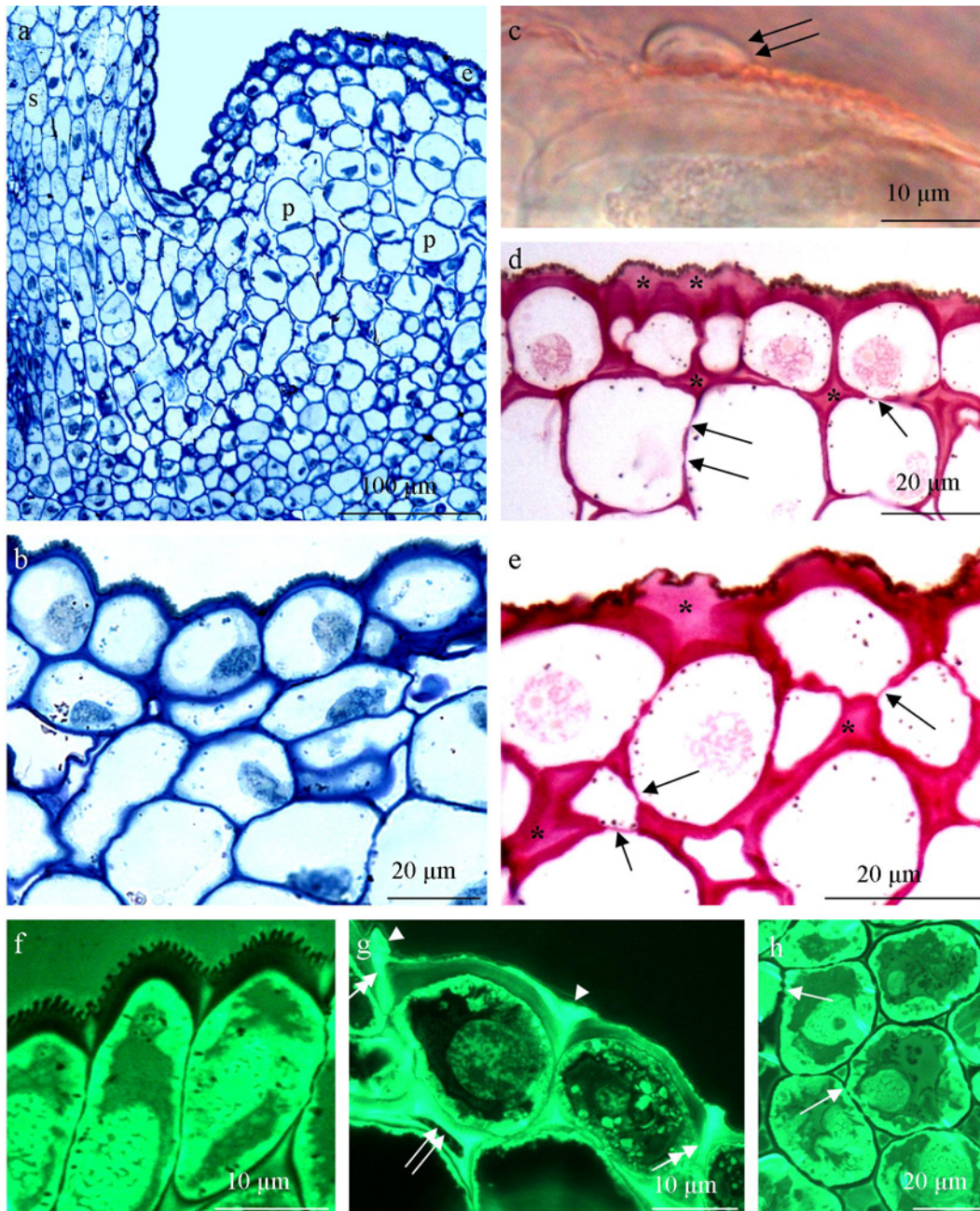


**Fig. 5** Longitudinal sections of the *Galanthus nivalis* nectary (**a–e** LM; **f–h** FM). **a** Nectary located by the style; visible small epidermal cells, large parenchymal cells (p) and small subglandular parenchymal cells. **b** Outer layers of the nectary tissues; epidermal cells with a thick outer cell wall and undulating cuticle and three layers of strongly vacuolated nectary parenchyma. **c** A part of nectary epidermal cells from fresh plant material; visible orange-stained cutinized layer of the outer cell wall with a drop of nectar on the surface (double arrow). **d,e** Nectary epidermal and parenchymal cells; visible pits in the walls (arrows) and secretion accumulated beneath the cuticle and in the intercellular spaces (asterisk). **f** Nectary epidermal cells, visible strongly thickened outer cell walls of the epidermis, large nuclei in the central part of the protoplasts. **g** Nectary epidermal cells (stage III), visible fluorescence of the nectar accumulated beneath the cuticle (arrowheads), along the radial epidermal walls (double headed arrow) and in the subepidermal intercellular spaces (two arrows). **h** Nectary parenchymal cells, visible strong vacuolation, large nuclei and pits in the cell walls (arrows). After treatment: toluidine blue (**a,b**), Sudan III (**c**), PAS reaction (**d,e**), auramine O, and using the FITC filter (**f–h**). e – epidermal cells; p – nectary parenchyma cells; s – style.

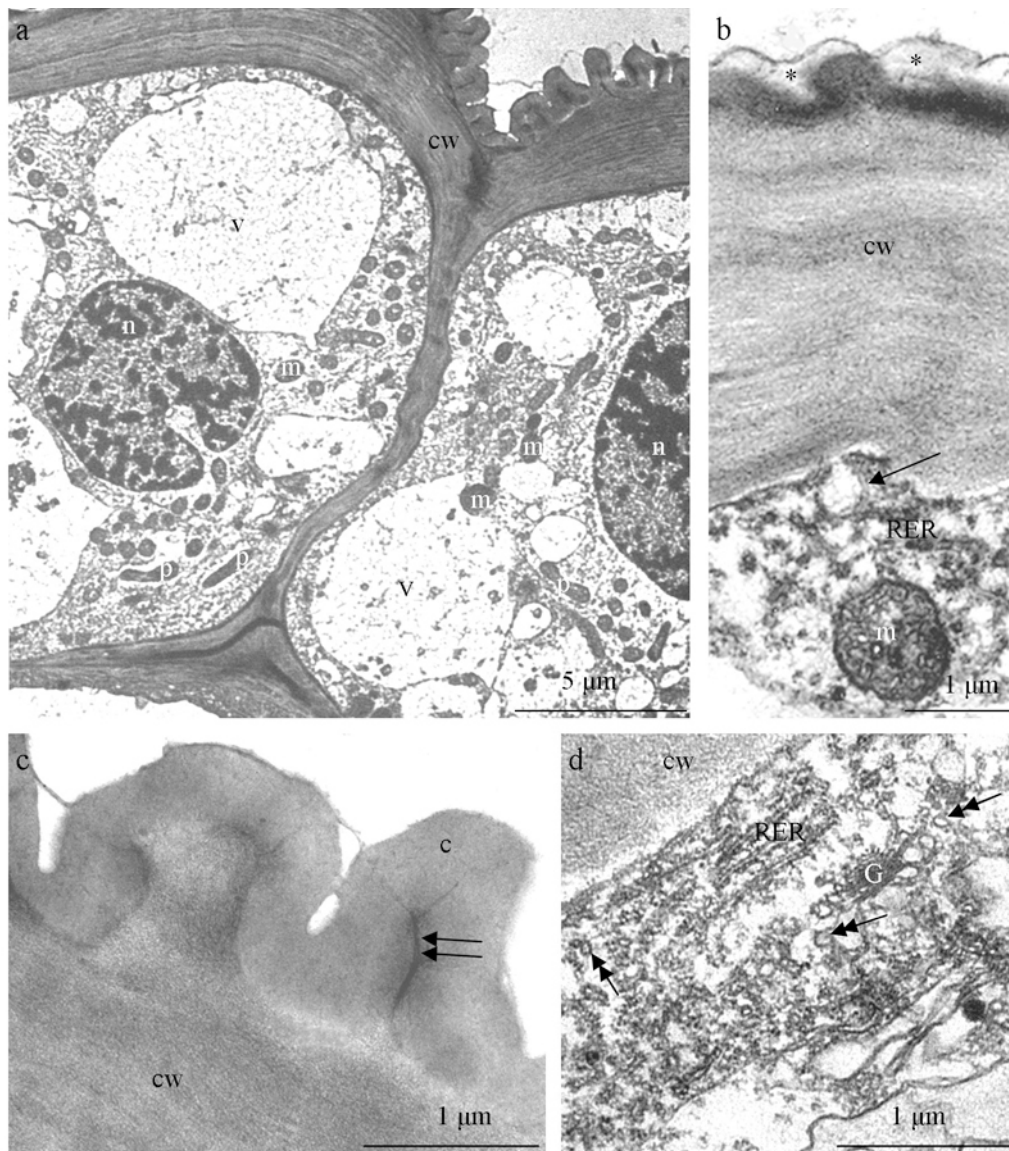


**Fig. 6** *Galanthus nivalis* nectary epidermal cells (stage II); TEM. **a** Cells with a thick outer cell wall, different-sized vacuoles, lobular cell nuclei, small plastids, and numerous mitochondria. **b** Fragment of the outer cell wall and parietal cytoplasm; a secretion-containing vesicle incorporated into the plasmalemma (arrow), mitochondrion, rough endoplasmic reticulum, subcuticular spaces (asterisks). **c** Fragment of the outer cell wall with a cuticle layer on the surface, micro-channels in the cuticle (two arrows). **d** Parietal cytoplasm with rough endoplasmic reticulum, Golgi apparatus, and numerous secretory vesicles (double headed arrows). c – cuticle; cw – cell wall; G – Golgi apparatus; m – mitochondria; n – nucleus; p – plastid; RER – rough endoplasmic reticulum.

undulation (Fig. 5d,e). In preparations from fresh plant material, a few light green plastids were observed in the epidermal cells. The cell nuclei in this tissue were characterized by large sizes and a lobular shape. They were located in the central part of the cell or close to the center (Fig. 5a,b,d,e, Fig. 6a). The cytoplasm was rich in granularities (Fig. 5b–e) which emitted distinct fluorescence (Fig. 5f,g).

#### Nectary parenchyma

The nectary parenchyma was characterized by large, highly vacuolated cells, whose cytoplasm and nuclei were most frequently located parietally (Fig. 5a,b,d). The parenchymal cell walls exhibited numerous simple pits (Fig. 5d,e,h). In many regions of the tissue, we observed large and very large intercellular spaces (Fig. 5a,b,e, Fig. 7a).

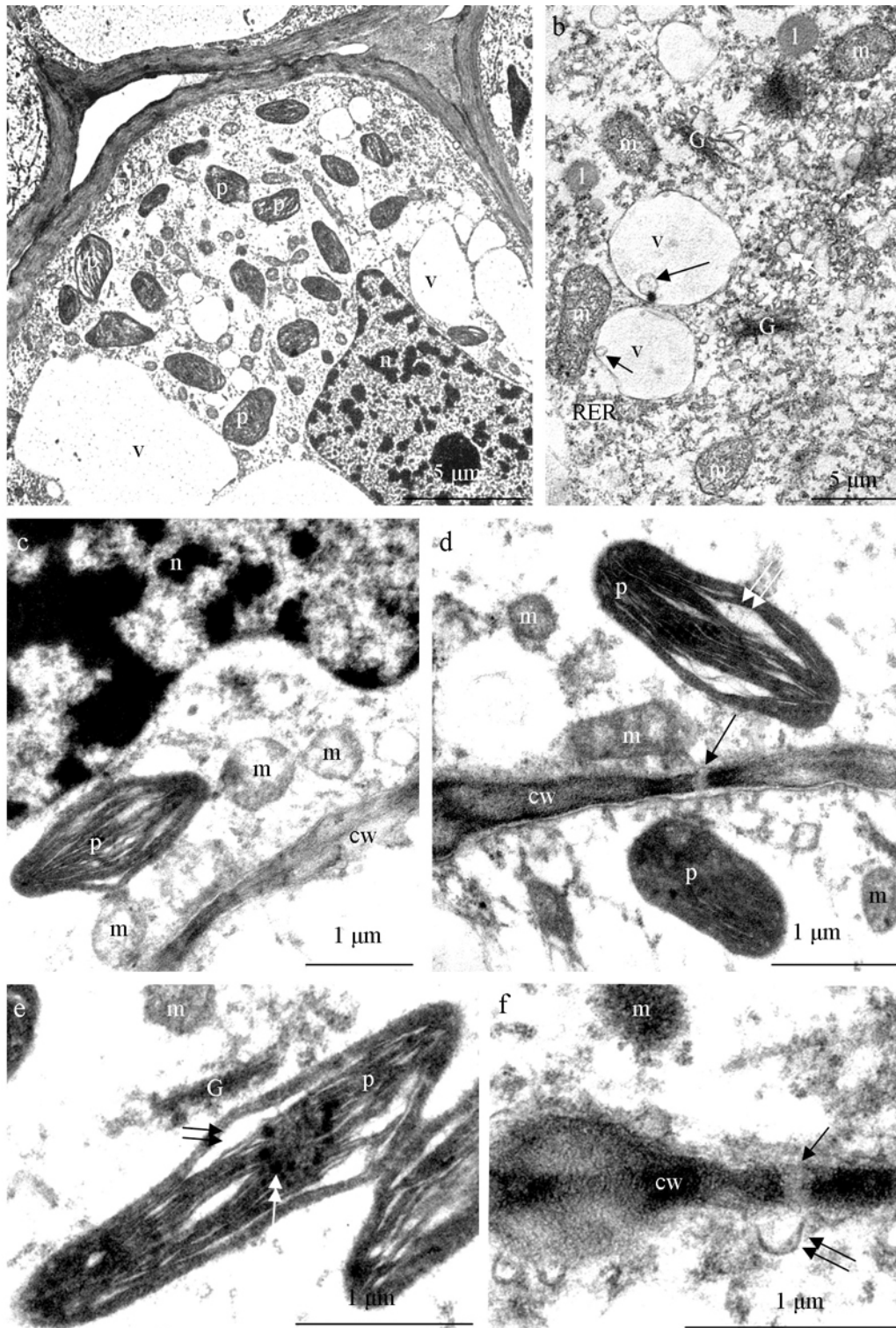


**Fig. 7** *Galanthus nivalis* nectary parenchymal cells in different stages (TEM). **a,b** Stage II; **d–f** Stage V. **a** Cell from the subepidermal layer with pleomorphic plastids, small vacuoles, numerous mitochondria, lobular cell nucleus, different-sized vacuoles, numerous endoplasmic reticulum profiles, and probably secretions in the intercellular space (asterisk; stage II). **b** Fragment of the cytoplasm with numerous Golgi apparatuses, secretory vesicles (arrow head), lipid bodies, rough endoplasmic reticulum, and vesicular structures (arrows) in the vacuoles (stage II). **c** Mitochondria arranged in groups close to the cell wall, the plastid, and the nucleus (stage V). **d,e** Plastids with electron-dense content, distinct thylakoids without the developed granal part and with small plastoglobules (double-headed arrow); many plastids exhibit bright regions emerging through thylakoid stratification (two arrows) or a convexity in the outer region of the plastid, two plastids in close contact (e), pits (arrow) in the walls (d; stage V). **f** Pits (arrow) in the cell walls (cw) and invaginations of the plasmalemma (double arrows; stage V). cw – cell wall; ER – endoplasmic reticulum; G – Golgi apparatus; l – lipid body; m – mitochondria; n – nucleus; p – plastid; RER – rough endoplasmic reticulum; v – vacuole.

The parenchyma cells contained small plastids. The PAS staining did not reveal starch grains before and during nectar secretion.

Using a variety of microscopic techniques, we observed the presence of nectar in the intercellular spaces, beneath the cuticle layer in the outer epidermal walls (Fig. 5d,e). In turn, induction of tissue fluorescence revealed secretion of significant amounts through the nectary epidermis radial walls (Fig. 5g).

### Nectary ultrastructure

**The nectary epidermis.** The epidermal cells had a 4–5  $\mu\text{m}$ -thick outer wall with a distinct, relatively thin, undulating cuticle layer reaching a thickness of ca. 0.47  $\mu\text{m}$  (Fig. 6a). The height of the cuticular striae (cuticle convexities) was 1.1–1.3  $\mu\text{m}$  (Fig. 6c). A very thin cuticular layer raised by nectar secreted was visible on the outer wall surface (Fig. 6b). The protoplasts of the epidermal cells were characterized by dense cytoplasm as well as numerous mitochondria and plastids. The lobular cell nuclei contained dark heterochromatin (Fig. 6a). The plastids had irregular shapes and often exhibited elongation. The mitochondria were located singly or in groups of several. Their internal structure exhibited distinct cristae (Fig. 6b). Numerous RER profiles and secretory vesicles were visible in various regions of the cytoplasm. Frequently, the RER systems were located near the cell walls (Fig. 6b,d). The Golgi apparatuses were accompanied by large dictyosomal vesicles (Fig. 6d). Local invagination of the plasmalemma gave rise to periplasmic spaces. Additionally, the fusion of secretory vesicles with the plasmalemma, accompanied by the release of nectar to the aforementioned space was also observed (Fig. 6b).

**The nectary parenchyma cells.** The walls of the glandular parenchyma cells were characterized by varied thickness (Fig. 7a). They contained numerous pits with plasmodesmata (Fig. 7d,f). Plasmalemma undulations formed periplasmic spaces (Fig. 7f). The intercellular spaces contained probably secretion (Fig. 7a). The electron-dense cytoplasm had multiple plastids and mitochondria. Irregular-shaped cell nuclei contained electron-dense chromatin and an osmophilic nucleolus (Fig. 7a,c). The mitochondria were arranged singly or in groups and had well-developed cristae. Numerous Golgi apparatuses and secretory vesicles were present in the cytoplasm (Fig. 7b). The plastids contained in the glandular parenchyma cells were usually elongated. They were characterized by a system of irregularly arranged thylakoids interspersed with transparent zones (Fig. 7c–e). A dark homogeneous stroma was visible in the plastids with a lesser degree of elongation (Fig. 7d). Some plastids contained dark plastoglobules associated with thylakoids. The closely located plastids were linked via convexities of the envelope portions and external parts of the plastids (Fig. 7e). We observed mitochondria connected with the plastid too (Fig. 7c). Additionally, lipid bodies were detected in the cytoplasm (Fig. 7b).

### Release of nectar onto the epidermis surface

The initial phase of nectar secretion was signaled by the appearance of tiny vesicles on the surface of the outer epidermal cell wall (Fig. 4c). Intense nectar secretion caused bulging (Fig. 4d) and detachment of the cuticle from the cell wall fragments located underneath and the formation of nectar-filled subcuticular spaces (Fig. 5d,e). The largest nectar-filled protuberances were observed in the areas of contact of two or more epidermal cells (Fig. 5e,g). Locally, the cuticle was strongly dilated and the cuticular striae were stretched (Fig. 5e). The release of nectar onto the surface of epidermal cells proceeded without cuticle rupture, as suggested by observation of nectar droplets above the cuticle layer (Fig. 5c). Significant amounts of nectar filling the spaces between the epidermis layer and glandular parenchyma were also visible after application of the PAS staining protocol (Fig. 5d,e), and by fluorescence microscopy. The nectar was also accumulated between the anticlinal walls of the epidermal cells, which were partially detached under the cuticle (Fig. 5g).

## Discussion

### Flowering

In Central Europe the onset of flowering of *G. nivalis* marks the beginning of the first phenological season [14] termed as early spring [1]. The time of blooming in early spring is greatly affected by the thermal conditions prevailing in the previous months [23]. In 2015 we recorded the beginning of *G. nivalis* flowering in Lublin on 18 February, while the end of flowering on 23 March (34 days). In 2012, on the other hand, according to Żuraw et al. [24] the flowering of this species in the same city lasted from 6 to 23 March (18 days). Maak and von Starch [14] demonstrated large differences in the time of blooming of *G. nivalis* in northern Germany at 74 study sites over the period 1971–1990. In their research, half of the data obtained showed that the beginning of *G. nivalis* flowering occurred before 28 February, whereas at other study sites it was recorded between the 38th and 85th day of the year. Budnikov and Kricsfalusy [25] report that in the East Carpathians the first *G. nivalis* flowers bloom from the end of February to the third 10 days of March, depending on the altitude (130–1320 m). The data given by the above-mentioned authors are in agreement with the *G. nivalis* flowering period reported for different regions of Poland (February–April) [3]. On the other hand, the beginning of flowering of this species is observed much earlier in the UK, as in the previous years it occurred already in January, on average 25 January [15].

### Breeding system

Our study shows that the lifespan of the *G. nivalis* flower was 31 days in 2015. It should be noted that it is an exceptionally long flowering duration for a flower. Chudzik and Śnieżko [26] found that the lifespan of unpollinated flowers of this species was 20–30 days, whereas pollinated flowers bloomed much shorter (3–15 days). In the case of the flowers observed in our study, no such relationship can be demonstrated as fruit formed from the ovary in all the flowers after the perianth had dropped off.

The flowers of *G. nivalis* can be considered to be homogamous, since we recorded stigma receptivity and pollen shed at the same time. This character indicates the possibility that the *G. nivalis* flower can be pollinated with its own pollen, which may also be confirmed by the very long flowering period and the long persistence of stigma receptivity as well as by the fact that fruit was set in all flowers. The outcrossing index (OCI), calculated according to the method given by Dafni [16], also shows that the flowers of *G. nivalis* are partially self-compatible.

Nevertheless, the characters clearly manifested in the flowers which indicate entomophily (a large perianth, scent, colored nectar guides, nectar) were also confirmed by the outcrossing index (outcrossing, demand for pollinators) and based on the determination of the outcrossing level (xenogamy). Chudzik et al. [27] revealed that when the flowers of *G. nivalis* were pollinated with their own pollen the number of seed-setting was half lower than in the case of pollination with foreign pollen.

### Apicultural value

Pollen and nectar production by plants that bloom earliest in the growing season is of great importance to bees and other insects seeking food already during early spring in order to replenish stores used during the winter [28]. The flowers of *G. nivalis* with their large stamens [6] produce significant amounts of pollen (4 mg), comparable to the mass of pollen in some species of the genus *Rosa* that produce an androecium of numerous stamens, e.g., *R. canina* [28]. The nectar contained in these flowers (2.66 mg), even though its amount is not evidence of abundant nectar production by this species, can be a very valuable source of early spring nectar for insects if these flowers occur in great numbers per unit of area.

### Location of the nectary

Our investigations show that the floral nectaries of *G. nivalis* are located at the top of the inferior ovary between the tepals and the style base. This location corresponds to the type of “gynoecial nectaries” and the group of “ovarian nectaries”, according to the data provided by Bernardello [10].

The literature data indicate that floral nectaries in monocotyledons represent two main types, i.e. septal and perigonal. Septal nectaries, e.g., present in many representatives of Asparagales and Liliales [10,12,29], are common in this class of plants [9]. The perigonal type comprises staminal and tepalar nectaries [30,31].

In plants of the family Amaryllidaceae, which produce an inferior ovary, septal nectaries are the prevalent type [11,12,29,31]. However, Rudall [29] reports that some species of this family are devoid of septal nectaries (e.g., *Cyrtanthus*). Bernardello [10] regards tepal nectaries as the characteristic type in Amaryllidaceae. In turn, Daumann [8] as well as Dafni and Werker [32] found in *Sternbergia* (Amaryllidaceae) three types of nectaries: tepal and staminal nectaries, apart from septal nectaries. In other representatives of Amaryllidaceae, various authors also report a dual location of the nectary in the flowers. Daumann [8] found that in species of the genus *Galanthus* two types of nectary occur: one on the inner tepals, while the other one, which is disk-shaped, at the base of the flower. Dahlgren et al. [9] also report that in the flowers of Galantheae tribus nectar is secreted in the distal part of the inner tepals and in the disk at the flower base. In our previous investigations focused on the micromorphology of elements of the *G. nivalis* perianth, we did not however find nectaries in the inner tepals [6]. Our study presented in this paper showed that the nectary gland in the flowers of the above-mentioned species is only located at the tip of the ovary, at the base of the stamens. Therefore, our results are only partially in agreement with the data contained in the papers of other authors concerning the location of the nectary in the flowers of *Galanthus nivalis*.

### Scent emission

Additionally, we drew attention to the more intense scent produced by the inner tepals than that of the outer tepals. We found that the structure of the inner tepals had the characteristics of the organs of odor-producing tissues (osmophores). We showed that their adaxial epidermis had numerous stomata and the upper surface was increased by the folds of the outer tissues, which facilitates the emission of an odorous secretion. Vogel [33] demonstrated that in some plants at the time of active emission of odorous compounds intense transpiration occurs during which stomata open wide. In *G. nivalis* the stomata in the epidermis of the tepals were mostly open.

Numerous stomata were earlier observed on the folded surface of the osmophores in *Amorphophallus rivieri* [34]. Kugler [7] also drew attention to the release of odorous compounds by the inner tepals of *Galanthus nivalis*. Numerous stomata occurred only on the adaxial ribbed surface that emitted a strong odor, while the abaxial surface was covered with different sized papillae. The results of our study concerning the presence of stomata in the adaxial epidermis of the inner tepals of *G. nivalis* are contradictory to the findings of Aschan and Pfanz [35] who report that stomata are lacking in the tepals of this species in both epidermal layers. However, the photosynthetic activity of the green parts of the tepals which emit a scent, as shown by the above-mentioned authors, even though it accounted for one fourth of the fully developed leaves, can be important for the supply of major substrates necessary in the metabolic pathway leading to the production of odorous substances.

### Nectary structure

The outer wall of the epidermal cells of the *G. nivalis* nectary was covered by an intensely undulating layer of the cuticle. Our observations carried out during the nectary secretory phase demonstrated that the cuticle in this species was strongly stretched by the secreted nectar; however, it did not rupture. In *G. nivalis* Kugler [7] also observed

stretching of the cuticle on the nectary surface by the accumulating nectar and did not find the cuticle to rupture, either. We observed microchannels in the cuticle. This may suggest that this layer in the nectaries is permeable to nectar. The occurrence of microchannels in the nectary cuticle has also been observed in other species by Nepi [36]. This author reported that in a majority of nectaries the cuticle was continuous and usually cracked in septal nectaries.

Numerous analyses of the anatomy of the nectary have demonstrated that the parenchyma of this gland is composed of small isodiametric cells [36–39]. In contrast, the *G. nivalis* nectary was found to consist of large parenchymal cells which were highly vacuolated during the nectar secretion phase. The tissue was characterized by the presence of large intercellular spaces. The fact of the occurrence of collenchyma in the subepidermal layer of the nectary in the flowers of the orchid *Maxillaria coccinea* can also indicate great diversity in the structure of nectariferous tissues [41].

The *G. nivalis* nectary was green whitish. In the plastids of the epidermal and parenchymal cells, we did not find granal thylakoids typical of chloroplasts. Our observations are in agreement with the data provided by Nepi [36] who claims that most typically small amounts of light reach the nectaries and, although they are green, their thylakoids and grana are underdeveloped. Lüttge [42] also found that green plastids of the nectaries often lacked granal thylakoids in which photosystem II is located.

The plastids in the *G. nivalis* nectaries observed in our study were characterized by the presence of electron-dense stroma, numerous unfused thylakoids and plastoglobules located in their close vicinity. This type of structure is similar to the structure of tubular chromoplasts, distinguished by various authors [43,44]. The plastids observed by us in the nectary cells are similar to some extent to chromoplasts occurring in the white parts of the tepals of this species investigated by Ščepánková and Hudak [5]. However, the unfused thylakoids in the plastids of the nectaries had a more regular arrangement than that described for the plastids in the tepals.

In the plastids of the *G. nivalis* nectaries, there were local protrusions that were in contact with the adjacent plastids. We also observed numerous mitochondria located in close vicinity of the plastids. Interconnections between plastids have been found in the cells of many plant species [44]. In cells of tomato, plastid complexes were found and they comprised the main parts of the plastid body and its stromules [45,46]. It has been shown that there is an exchange of protein molecules between plastids of higher plants [47]. The studies of other authors reveal that plastids and mitochondria located in close vicinity to one another can exchange metabolites [48]. The above-cited authors suggest that plastids and mitochondria may have a synergistic effect on plant growth and development.

The protrusions found in the plastids of the *G. nivalis* nectaries can also be adaptations to lower temperature conditions. Gielwanowska et al. [49] as well as Gielwanowska and Szczuka [50] considered different deformations (pockets, lacunae) in plastids of the leaves of Antarctic plants to be adaptations to extreme conditions. We observed spherical osmophilic inclusions in the parenchymal cells of the nectaries. Similar inclusions of various sizes were observed in Antarctic plants by the above-mentioned authors.

We observed numerous plastids, mitochondria, dictyosomes, ER cisterns, and abundant vesicles in the epidermal and parenchymal cells of the *G. nivalis* nectary. In many sites, the vesicles were fused with the plasmalemma, which may indicate nectar secretion in the granulocrine system. Granulocrine nectar secretion has been demonstrated in many other monocotyledons species of the genera *Asphodelus*, *Brassavola*, *Musa*, *Platanthera*, and *Strelitzia* [51–53].

## References

1. Podbielkowski Z. Geografia roślin. Warszawa: WSiP; 1991.
2. Nekovar J, Dalezios N, Koch E, Kubin E, Nejedlik P, Niedzwiedz T, et al. The history and current status of plant phenology in Europe. Helsinki: Vammalan Kirjapaino Oy; 2008.

3. Piękoś-Mirkowa H, Mirek Z. Rośliny chronione. Warszawa: Multico; 2003.
4. Rozporządzenie Ministra Środowiska z dnia 9 października 2014 r. w sprawie ochrony gatunkowej roślin. Dz. U. z 2014 r., poz. 1409.
5. Štěpánková I, Hudák J. Leaf and tepal anatomy, plastid ultrastructure and chlorophyll content in *Galanthus nivalis* L. and *Leucojum aestivum* L. Plant Syst Evol. 2004;243(3–4):211–219. <http://dx.doi.org/10.1007/s00606-003-0086-y>
6. Weryszko-Chmielewska E, Chwil M. Ecological adaptations of the floral structures of *Galanthus nivalis* L. Acta Agrobot. 2010;63(2):41–49. <http://dx.doi.org/10.5586/aa.2010.031>
7. Kugler H. Blütenökologie. Stuttgart: Gustav Fischer Verlag; 1970.
8. Daumann E. Das Blütennektarium der Monocotyledonen unter besonderer Berücksichtigung seiner systematischen und phylogenetischen Bedeutung. Feddes Repert. 1970;80:463–590. <http://dx.doi.org/10.1002/fedr.19700800702>
9. Dahlgren RMT, Clifford HT, Yeo PF. The families of the monocotyledons. Structure, evolution, and taxonomy. Berlin: Springer; 1985. <http://dx.doi.org/10.1007/978-3-642-61663-1>
10. Bernardello G. A systematic survey of floral nectaries. In: Nicolson SW, Nepi M, Pacini E, editors. Nectaries and nectar. Dordrecht: Springer; 2007. p. 19–128. [http://dx.doi.org/10.1007/978-1-4020-5937-7\\_2](http://dx.doi.org/10.1007/978-1-4020-5937-7_2)
11. Chwil M. Ecology of flowers and morphology of pollen grains of selected *Narcissus* varieties (*Narcissus pseudonarcissus* L. × *Narcissus poëticus* L.). Acta Agrobot. 2006; 59:107–122. <http://dx.doi.org/10.5586/aa.2006.011>
12. Endress PK. Major evolutionary traits of monocot flowers. In: Rudall PJ, Cribb PJ, Cutler DF, Humphries CJ, editors. Monocotyledons: systematics and evolution. Kew: Royal Botanic Gardens; 1995. p. 43–79.
13. Szafer W, Wojtusiakowa H. Kwiaty i zwierzęta: zarys ekologii kwiatów. Warszawa: Państwowe Wydawnictwo Naukowe PWN; 1969.
14. Maak K, von Storch H. Statistical downscaling of monthly mean air temperature to the beginning of flowering of *Galanthus nivalis* L. in northern Germany. Int J Biometeorol. 1997;41:5–12. <http://dx.doi.org/10.1007/s004840050046>
15. Sparks TH, Jeffree EP, Jeffree CE. An examination of the relationship between flowering times and temperature at the national scale using long-term phenological records from the UK. Int J Biometeorol. 2000;44:82–87. <http://dx.doi.org/10.1007/s004840000049>
16. Dafni A. Pollination ecology: a practical approach. Oxford: Oxford University Press; 1992.
17. Jabłoński B. Metodyka badań obfitości nektarowania kwiatów i oceny miododajności roślin. Puławy: Oddział Pszczelnictwa Instytutu Sadownictwa i Kwiaciarstwa; 2003.
18. Warakomska Z. Badania nad wydajnością pyłkową roślin. Pszczelnicze Zeszyty Naukowe. 1972;16:63–90.
19. Jensen WA. Botanical histochemistry: principle and practice. San Francisco, CA: W.H. Freeman; 1962.
20. Feder N, O'Brien TP. Plant microtechnique: some principles and new methods. Am J Bot. 1968;55:123–142. <http://dx.doi.org/10.2307/2440500>
21. Wędzony M. Mikroskopia fluorescencyjna dla botaników. Cracow: Department of Plant Physiology, Polish Academy of Sciences; 1996. (Monografie; vol 5).
22. Reynolds ES. The use of lead citrate at high pH as an electron-opaque stain in electron microscopy. J Cell Biol. 1963;17:208–212. <http://dx.doi.org/10.1083/jcb.17.1.208>
23. Defila C. Pflanzenphänologischer Kalender ausgewählter Stationen in der Schweiz. Zürich: Schweizerische Meteorologische Anstalt; 1992.
24. Żuraw B, Chyżewska R, Rysiak K, Chernetskyy M. Blooming biology and visitation by pollinating insects of the snowdrop (*Galanthus nivalis* L.) flowers. In: Bogucka-Kocka A, Kocki J, Sowa I, editors. Book of abstracts: “Plant-the source of research material” – 2nd International Conference and Workshop; 2012 Oct 18–20; Lublin, Poland. Lublin: Polihymnia; 2012. p. 374.
25. Budnikov G, Kricsfalusy V. Bioecological study of *Galanthus nivalis* L. in the East Carpathians. Thaiszia Journal of Botany. 1994;4:49–75.
26. Chudzik B, Snieżko R. Calcium ion presence as a trait of receptivity in tenuinucellar ovules of *Galanthus nivalis* L. Acta Biol Crac Ser Bot. 2003;45(1):133–141.

27. Chudzik B, Snieżko R, Szaub J. Biology of flowering of *Galanthus nivalis* L. (Amaryllidaceae). *Ann Univ Mariae Curie-Skłodowska EEE Horti* 2002;10:1–10.
28. Maurizio A, Grafl I. *Das Trachtpflanzenbuch*. München: Ehrenwirth Verlag; 1969.
29. Rudall P. Homologies of inferior ovaries and septal nectaries in monocotyledons. *Int J Plant Sci*. 2002;163(2):261–276. <http://dx.doi.org/10.1086/338323>
30. Dahlgren RMT, Clifford HT. *The monocotyledons: a comparative study*. London: Academic Press; 1982.
31. Smets EF, Ronse Decraene LP, Caris P, Rudall PJ. Floral nectaries in monocotyledons: distribution and evolution. In: Wilson KL, Morrison DA, editors. *Monocots: systematics and evolution*. Melbourne: CSIRO; 2000: p. 230–240.
32. Dafni A, Werker E. Pollination ecology of *Sternbergia clusiana* (Ker-Gawler) Spreng. (Amaryllidaceae). *New Phytol*. 1982;91:571–577. <http://dx.doi.org/10.1111/j.1469-8137.1982.tb03335.x>
33. Vogel S. *The role of scent glands in pollination on the structure and function of osmophores*. New Delhi: A Merind Publishing Co; 1990.
34. Weryszko-Chmielewska E, Stpiczyńska M. Osmophores of *Amorphophallus rivieri* Durieu (Araceae). *Acta Soc Bot Pol*. 1995;64(2):121–229. <http://dx.doi.org/10.5586/asbp.1995.016>
35. Aschan G, Pfanz H. Why snowdrop (*Galanthus nivalis* L.) tepals have green marks. *Flora*. 2006;8:623–632. <http://dx.doi.org/10.1016/j.flora.2006.02.003>
36. Nepi M. Nectary structure and ultrastructure. In: Nicolson SW, Nepi M, Pacini E, editors. *Nectaries and nectar*. Dordrecht: Springer. 2007. p. 129–166. [http://dx.doi.org/10.1007/978-1-4020-5937-7\\_3](http://dx.doi.org/10.1007/978-1-4020-5937-7_3)
37. Weryszko-Chmielewska E, Chwil M. Morphological features of the nectary and of the pollen grains and the foraging value of the flowers of yellow azalea (*Rhododendron luteum* Sweet). *Journal of Apicultural Science*. 2005;422:5–12.
38. Weryszko-Chmielewska E, Chwil M. Micromorphology of nectaries of *Rhododendron catawbiense* Michx. at different flower development stages. *Acta Agrobot*. 2007;60(2):15–22. <http://dx.doi.org/10.5586/aa.2007.025>
39. Weryszko-Chmielewska E, Chwil M. Micromorphology of the epidermis of the floral nectary of *Rhododendron japonicum* (A. Gray) JV Suringar ex EH Wilson. *Acta Agrobot*. 2007;60(1):45–53. <http://dx.doi.org/10.5586/aa.2007.005>
40. Chwil S, Chwil M. Micromorphology and ultrastructure of the floral nectaries of *Polemonium caeruleum* L. (Polemoniaceae). *Protoplasma*. 2012;249(4):1059–1069. <http://dx.doi.org/10.1007/s00709-011-0341-y>
41. Stpiczyńska M, Davies KL, Gregg A. Nectary structure and nectar secretion in *Maxillaria coccinea* (Jacq.) L.O. Williams ex Hodge (Orchidaceae). *Plant Syst Evol*. 2003;238(1):119–126. <http://dx.doi.org/10.1093/aob/mch008>
42. Lüttge U. Green nectaries: the role of photosynthesis in secretion. *Bot J Linn Soc*. 2013; 173:1–11. <http://dx.doi.org/10.1111/boj.12066>
43. Woźny A, Michejda J, Ratajczak L. *Podstawy biologii komórki roślinnej*. Poznań: Wydawnictwo Naukowe Uniwersytetu im. Adama Mickiewicza; 2001.
44. Evert RF. *Esau's plant anatomy: meristems, cells, and tissues of the plant body: their structure, function, and development*. 3rd ed. Hoboken, NJ: John Wiley & Sons, Inc; 2006. <http://dx.doi.org/10.1002/0470047380>
45. Pyke KA, Howells CA. Plastid and stromule morphogenesis in tomato. *Ann Bot*. 2002;90:559–566. <http://dx.doi.org/10.1093/aob/mcf235>
46. Waters MT, Fray RG, Pyke KA. Stromule formation is dependent upon plastids size, plastid differentiation status and the density of plastids within the cell. *Plant J*. 2004;39:655–667. <http://dx.doi.org/10.1111/j.1365-313X.2004.02164.x>
47. Köhler RH, Cao J, Zipfel WR, Webb WW, Hanson MR. Exchange of protein molecules through connections between higher plant plastids. *Science*. 1997;276:2039–2042. <http://dx.doi.org/10.1126/science.276.5321.2039>
48. Inaba T, Ito-Inaba Y. Versatile roles of plastids in plant growth and development. *Plant Cell Physiol*. 2010;51:1847–1853. <http://dx.doi.org/10.1093/pcp/pcq147>
49. Giełwanowska I, Szczuka E, Bednara J, Górecki R. Anatomic features and ultrastructure of *Deschampsia antarctica* Desv. Leaves from different growing habitats. *Ann Bot*. 2005;96:1109–1119. <http://dx.doi.org/10.1093/aob/mci262>
50. Giełwanowska I, Szczuka E. New ultrastructural features of organelles in leaf cells of

- Deschampsia antarctica* Desv. Polar Biol. 2005;28:951–955. <http://dx.doi.org/10.1007/s00300-005-0024-2>
51. Fahn A. Secretory tissues in plants. New York, NY: Academic Press; 1979.
  52. Kronstedt-Robards E, Robards AW. Exocytosis in gland cells. In: Hawes CR, Coleman JOD, Coleman DE, editors. Endocytosis, exocytosis and vesicle traffic in plants. Cambridge: Cambridge University Press. 1991. p. 199–232.
  53. Weryszko-Chmielewska E, Sawidis T, Piotrowska K. Anatomy and ultrastructure of floral nectaries of *Asphodelus aestivus* Brot. (Asphodelaceae). Acta Agrobot. 2006;59:29–42. <http://dx.doi.org/10.5586/aa.2006.059>